Lab on a Chip

RSC Publishing

TECHNICAL INNOVATION

View Article Online
View Journal

Ultra-localized single cell electroporation using silicon nanowires†

Cite this: DOI: 10.1039/c2lc40837f

Nima Jokilaakso,‡[a] Eric Salm,‡[bf] Aaron Chen,[c] Larry Millet,[df] Carlos Duarte Guevara,[df] Brian Dorvel,[ef] Bobby Reddy Jr.,[df] Amelie Eriksson Karlstrom,[a] Yu Chen,[g] Hongmiao Ji,[g] Yu Chen,[g] Ratnasingham Sooryakumar[c] and Rashid Bashir*[bdf]

Received 24th July 2012,
Accepted 25th October 2012

DOI: 10.1039/c2lc40837f

www.rsc.org/loc

Analysis of cell-to-cell variation can further the understanding of intracellular processes and the role of individual cell function within a larger cell population. The ability to precisely lyse single cells can be used to release cellular components to resolve cellular heterogeneity that might be obscured when whole populations are examined. We report a method to position and lyse individual cells on silicon nanowire and nanoribbon biological field effect transistors. In this study, HT-29 cancer cells were positioned on top of transistors by manipulating magnetic beads using external magnetic fields. Ultra-rapid cell lysis was subsequently performed by applying 600–900 mV_{pp} at 10 MHz for as little as 2 ms across the transistor channel and the bulk substrate. We show that the fringing electric field at the device surface disrupts the cell membrane, leading to lysis from irreversible electroporation. This methodology allows rapid and simple single cell lysis and analysis with potential applications in medical diagnostics, proteome analysis and developmental biology studies.

Introduction

Analysis of cellular content, such as proteins and nucleic acid molecules typically requires *a priori* cell lysis by rupture of the cell membrane. This can be achieved by chemical,[1] electrical,[2,3] enzymatic,[4] mechanical[5–8] or thermal[9,10] means. Each technique presents unique advantages and disadvantages that must be considered to ensure compatibility with downstream analysis.[11] For example, conventional thermal lysis is a bulk and non-specific process that leads to breakdown of cell membranes and cell compartments, and can cause denaturation of biomolecules such as proteins and nucleic acids. This can lead to degradation of analytes such as proteins, thus hindering integration of thermal cell lysis with analysis of cellular content.[12]

An alternative lysis methodology is cellular electroporation, which has been discussed thoroughly in the literature.[13] In electroporation procedures, an applied electric field creates a potential across the cell membrane, known as the transmembrane potential (TMP). Once this potential exceeds a certain threshold, ~0.2–1.0 V, pores will form in the cellular membrane.[14] Variations in the size and number of pores formed depends on the duration and strength of the applied electric field as well as the cell type, developmental stage, medium and cellular dimensions. Depending on their size and number, these pores will either reseal (termed reversible electroporation) or they will remain open resulting in irreversible electroporation. In irreversible electroporation, cellular contents are released and the cell dies. This technique can allow for molecular analysis of released content with minimal induced damage. Since the first single cell electroporation in 1998,[15] several methods for single cell electroporation have been developed[16] utilizing platforms such as microfabricated chips[17,18] and vertical nanopillars.[19]

We have previously demonstrated localized fringing electric fields at a transistor's surface using an AC voltage mediated strategy.[20–22] In the current work, we show through experiments and simulations that the electric fields generated directly above the device enable electroporation at applied voltages of less than 1 V. In this approach, the electric field is highly localized at the nanometre scale above the device surface, which enables specific, single cell lysis.

In order to electroporate single cells, cells must be individually targeted and positioned. A variety of methods have been used to controllably position cells including patterning,[23] fluidic traps and wells,[24] optical traps,[25] dielectrophoresis,[9] and others.[26] The method used in this study incorporates a label-free and trap-less technique where magnetic beads are rolled to

[a]Division of Molecular Biotechnology, Royal Institute of Technology (KTH), Stockholm, 106 91, Sweden
[b]Department of Bioengineering, University of Illinois Urbana-Champaign, Urbana, 61801, Illinois, USA. E-mail: rbashir@illinois.edu; Fax: +1-217-244-6375; Tel: +1-217-333-3097
[c]Department of Physics, Ohio State University, Columbus, 43210, Ohio, USA
[d]Department of Electrical and Computer Engineering, University of Illinois Urbana-Champaign, Urbana, 61801, Illinois, USA
[e]Department of Biophysics, University of Illinois Urbana-Champaign, Urbana, 61801, Illinois, USA
[f]Micro and Nanotechnology Lab, University of Illinois Urbana-Champaign, Urbana, 61801, Illinois, USA
[g]Institute of Microelectronics, Singapore A*STAR (Agency for Science, Technology and Research), Singapore, 117685, Singapore

† Electronic supplementary information (ESI) available: Additional figures and a video. See DOI: 10.1039/c2lc40837f

‡ Equal contribution.

push and pull untethered or non-specifically-bound cells into a desired position.[27–29] This technique is attractive as it does not require the transparent substrates needed for optical tweezers or the high voltages on chip and strict control of media conductivity required for dielectrophoresis.

In this paper, we demonstrate integration of magnetic manipulation techniques with a robust cell lysis technique. By using field effect transistors to apply an electric field to cells, we enable a gentle and specific cell lysis with potential for field effect sensing of released cellular components. This would enhance the usability and portability of lab-on-a-chip devices by minimizing loss of biological molecules.[30] We envision this system being used in single cell analysis studies that focus on cell-to-cell variation within a population.

Materials and methods

Chip fabrication

Fabrication details of the silicon field effect devices using a Silicon on Insulator (SOI) wafer have been described elsewhere[31] (see Fig. 1 for device architecture). Silicon nanowires (SiNW) and silicon nanoribbons (SiNR) were used. The SiNWs had a width of 50–100 nm and a thickness of 30 nm whereas the SiNRs had a thickness of 50 nm, but a width of 2 μm.

Surface preparation

To prevent premature cellular adhesion, the surfaces were passivated using an organosilane monolayer. The process consisted of an oxygen plasma treatment for 2 min, then, 50 μl of 5% 3-aminopropyldimethylethoxysilane, APDMS (Gelest Inc.) in toluene is pipetted onto the reactive surface and incubated for 15 min. The surface is rinsed with toluene, methanol, DI water and wiped with a microfiber swab. The device was then treated with trypsin–EDTA (0.25% trypsin–0.53 mM EDTA in Hank's Balanced Salt Solution (HBSS) without calcium and magnesium) before cell addition to further reduce cell adhesion. Excess trypsin–EDTA was rinsed off with DI water prior to device usage.

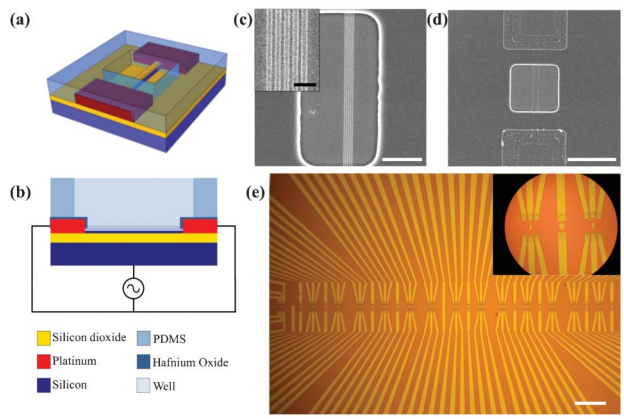

Fig. 1 (a) A cross section of the device is shown. The release window above the nanoribbon is 20 × 20 μm. (b) The electrical schematic is shown with PDMS above the device. (c) An SEM image of a grouping of 5 nanowires. (d) An SEM image of a nanoribbon device. (e) An array of transistors with both nanowires and nanoribbons. Scale bars are (c) 5 μm, inset 400 nm, (d) 20 μm, (e) 200 μm.

HT-29 cell culture and preparation

HT-29 cells (human colon carcinoma, ATCC # HTB-38™) were used throughout the study and prepared using standard cell culture conditions with Dulbecco's Modified Eagle Medium (DMEM) (Invitrogen corp, Carlsbad, CA), supplemented with 10% Fetal Bovine Serum (FBS) (Sigma Aldrich, St. Louis, MO) and 1% penicillin–streptomycin.

Cell positioning with magnetic beads

Cell positioning on devices utilized the programmability of magnetic field routines for magnetic manipulation of 7.9 μm COOH-modified COMPEL magnetic microspheres from Bangs Laboratories, Inc. (Fig. 2(a) and (b)). Details on this setup and its operation can be found in prior work.[27–29] To ensure stable measurements, the positioned cells were allowed to adhere to the device surface for 30 min prior to lysis.

Cell lysis

The setup used was described in prior work, but at higher voltages.[20–22] In this study, voltages at 10 MHz and up to 900 mV_{pp} were applied between the shorted source–drain and the back gate of a transistor, shown in a schematic representation (Fig. 1 (a) and (b)).

Live-dead assay

A live-dead assay for monitoring cell membrane integrity was adapted from Privorotskaya *et al.*[10] Propidium iodide (PI), a membrane impermeable dye, and $DiOC_6(3)$, a membrane dye, from Sigma Aldrich were used. Upon break down of the cell membrane, PI enters the cell and intercalates with the cellular DNA. An increase in PI fluorescence was used to determine cell lysis. Lysed and intact cells were also fixed using a similar protocol to Privorotskaya *et al.*[10]

Results and discussion

Cell positioning characterization

The two variable parameters of the magnetic positioning system, frequency (Hz) and strength (Gauss), of the rotating magnetic field were characterized for the magnetic beads to optimize speed and control of the movement of cells. With optimization of the surface preparation as well as the applied field strength and frequency, magnetic beads could be reliably used to position cells. As shown

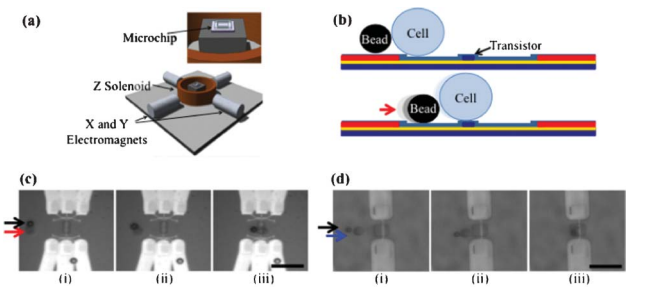

Fig. 2 (a) Schematic of the magnetic bead setup. The electromagnets generate a magnetic field, which rolls magnetic beads across the chip surface. (b) The beads are used to push the cells into position above the transistor. (c) An MCF-7 cell (red arrow) is moved from left to right by a bead (black arrow) to a position over a set of nanowires (in ~2 s, shown over the course of three images). (d) An HT-29 cell (blue arrow) is moved from left to right by a bead (black arrow) and positioned over a nanoribbon. Scale bars in (c) and (d) are 40 μm.

in Fig. 2(c) and (d), cells of various types could be reliably positioned directly above the transistors for later lysis. Video SV1 (ESI†) shows the speed of movement of a bead and positioning of an HT-29 cell on a device.

Cell electroporation characterization

The membrane dye, $DiOC_6(3)$, and the membrane-impermeable dye, PI, were added to the solution of cell media containing HT-29 cells and magnetic beads. Bright field and fluorescent images of cells positioned on devices were taken before and after an application of a 10 MHz pulse of 1200 mV_{pp} for 1 min and during 60 min incubations (Fig. 3(a) and (b)). The time course of fluorescence (Fig. 3(b)) shows PI (red) fluorescence increasing after voltage application, which implies degradation of the cellular membrane. SEM images of an intact cell and a lysed cell were also taken (Fig. 3(c) and (d)). The SEM of the lysed cell shows significant breakdown of the cell membrane from the applied signal. Fig. S1 (ESI†) shows the highly localized nature of this method. Only a cell located directly on top of the transistor is lysed, while cells immediately adjacent are unharmed. Experiments to determine the lysis threshold were also carried out. Voltages of 300, 600, and 900 mV_{pp} were applied. 0% (n = 10) of cells at 300 mV_{pp} for 1 min were lysed, 83% (n = 12) of cells at 600 mV_{pp} for as little as 2 ms were lysed, and 100% (n = 5) were lysed at 900 mV_{pp} for 1 s. The threshold for lysis is likely between 300 and 600 mV_{pp}.

Lysis mechanism

We found that applied voltages above 600 mV_{pp} induced irreversible electroporation. To understand this threshold, we used a model (eqn (1)) developed by Grosse and Schwan in order to calculate the TMP induced by alternating electric fields.[32]

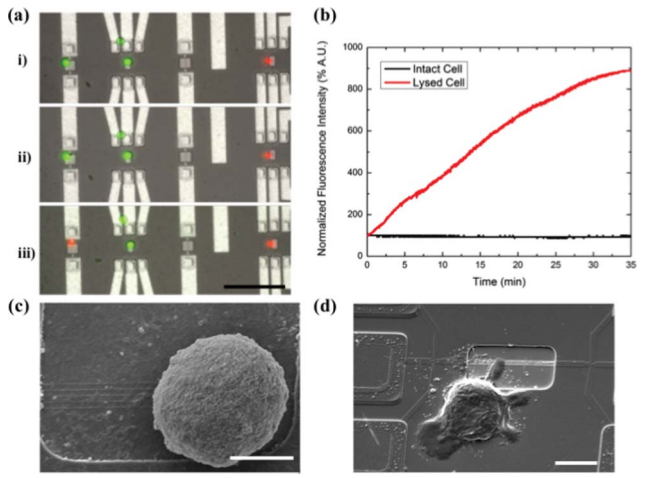

Fig. 3 (a) An MCF-7 cell on the far left nanoribbon is lysed *via* an applied signal of 600 mVpp, 10 MHz for 2 ms. Two live cells on or near the second nanoribbon from the left as well as one already dead cell on the far right are shown as reference. Images (i–iii) show $DiOC_6(3)$ (green) and PI (red) fluorescence signals from these cells. (i) Shows the cell before applied voltage. (ii) Shows immediately after the signal was applied. (iii) After 20 min, PI fluorescence in the cell has increased, implying cell death. The control cell on the nanowire to the right shows no PI increase over the duration of the experiment. (b) Shows the time course of PI fluorescence increase for an intact cell and a lysed cell. (c) An SEM image of an intact cell. (d) An HT-29 cell that has been lysed by the applied signal to a nanowire is shown. Scales bars are (a) 100 μm, (c) 5 μm, (d) 10 μm.

$$\Delta \mathrm{TMP} = \frac{\frac{3}{2} ER\cos(\theta)}{1 + i\omega RC_m\left(\rho_i + \frac{\rho_a}{2}\right)} \quad (1)$$

Using electric field calculations from simulations, and constants from HT-29 cells and the media used (Table 1, ESI†), the TMP for a range of voltages was calculated (Fig. 4). The calculations show that, directly at the device surface, a 300 mV_{pp} signal creates a TMP of 1.21 V. This value exceeds the expected threshold for irreversible electroporation of 0.2–1.0 V;[14] however, cell lysis was not observed. To explain this discrepancy between experimental *vs.* theoretical results, it is important to examine the role distance plays in the electric field strength above the device. Fig. 4 shows that the calculated TMP created by the applied signal decays rapidly above the device surface. Within 10 nm of the device surface, the TMP will decrease by almost 67%. In our protocol, the cell was allowed to settle down and adhere to the device surface. As a cell adheres to a surface, an extracellular matrix consisting of a few layers of proteins is formed.[33] This layer can vary greatly in thickness, but should be in the order of ~10 nm.[34] At this distance, a 300 mV_{pp} applied signal results in a TMP of 0.5 V. This value is on the lower end of TMP that will result in electroporation. However, the 600 mV_{pp} signal still provides a TMP of 1.05 V, which is high enough for electroporation to occur.

To confirm that the cell lysis was due primarily to electroporation, the temperature profile above the device was interrogated to determine whether the voltages used for cell lysis would generate any joule heating or AC heating. We used a dsDNA molecule, modified with a FRET acceptor on one strand and a donor on the other strand, which was added to pure cell culture media. This dsDNA FRET construct was designed to denature at 70 °C and upon denaturation, the observed fluorescence would increase due to separation of the FRET donor and acceptor pair. The voltage was increased in 2.4 V_{pp} increments every 10 s up to 100 V_{pp}. Measurement of three zones extending away from the device showed no observed fluorescence increase from heating at the low voltages used for cell lysis (Fig. S2, ESI†). Fluorescence from DNA

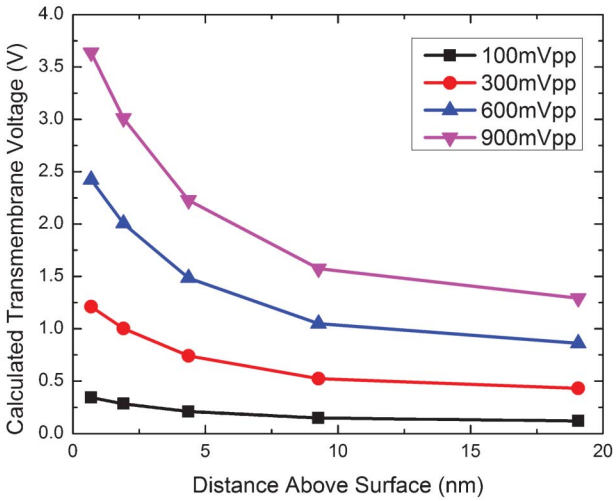

Fig. 4 The TMP for a range of applied voltages was calculated. The TMP decays with decreasing electric field strength moving away from the device surface.

denaturation only increased above 64 V_{pp}, which corresponds to values reported in previous studies using this technique.[21]

Current–voltage characterization was also performed before and after electroporation pulse application to ensure the applied signal did not damage the device's electrical characteristics (see Fig. S3, ESI†). The results show that the threshold voltage and saturation current are only slightly altered; however, the device retained transistor characteristics and had low current leakage post-lysis.

Conclusions

Here we present a novel method for lysis of single cells positioned directly above a field effect transistor. This technique has the potential to enable many applications that require specific, localized cell lysis on a biosensing platform. We describe a simple method for releasing biological components from the cell, which reduces the impact on molecule stability from thermal, chemical, or mechanical degradation. Label-free and trap-less magnetic manipulation of cells especially overcomes the need for transparent substrates in optical tweezer techniques; the need for microfluidic trapping techniques; and the need for high voltages and low media conductivity in dielectrophoresis-based trapping of cells. This methodology can be applied to a wide variety of biological studies that focus on single cell *vs.* cell population analysis.

Acknowledgements

The authors thank Lauren Yang for editing the manuscript, Anand Harvind, Samuel Stuard and Atul Bharde for assistance with the magnetic manipulation. N.J. acknowledges a Gålöstiftelsen scholarship for higher studies. R.S. and R.B. acknowledge the support of the NSF NSEC at OSU grant number EEC-0914790. R.S. acknowledges funding from the U.S. Army Research Office under contract W911NF-10-1-0353. R.B. also acknowledges funding support from a cooperative agreement with Purdue University and the Agricultural Research Service of the United States Department of Agriculture, project number 1935-42000-035, and a sub-contract to the University of Illinois at Urbana-Champaign. We also acknowledge support from NIH Grant R01-CA20003 and NSF I/IUCRC CABPN (Center for Agricultural, Biomedical and Pharmaceutical Nanotechnology) Grant at UIUC.

Author contributions: R.S. and R.B. designed the experiments. N.J., E.S., A.C., B.R., C.D. and L.M. performed experiments. N.J., E.S. and R.B. analysed data. B.D., Y.C., H.J., and C.Y. fabricated devices. E.S. and R.B. wrote the paper. All authors discussed the results and commented on the manuscript.

References

1 D. Irimia, R. G. Tompkins and M. Toner, *Anal. Chem.*, 2004, **76**, 6137–6143.
2 J. T. Nevill, R. Cooper, M. Dueck, D. N. Breslauer and L. P. Lee, *Lab Chip*, 2007, **7**, 1689–1695.
3 M. Khine, A. Lau, C. Ionescu-Zanetti, J. Seo and L. P. Lee, *Lab Chip*, 2005, **5**, 38–43.
4 O. Salazar and J. A. Asenjo, *Biotechnol. Lett.*, 2007, **29**, 985–994.
5 J. Kim, J. W. Hong, D.-P. Kim, J. H. Shin and I. Park, *Lab Chip*, 2012, **12**, 2914–2921.
6 M. Wurm and A. P. Zeng, *Lab Chip*, 2012, **12**, 1071–1077.
7 H. Hoefemann, S. Wadle, N. Bakhtina, V. Kondrashov, N. Wangler and R. Zengerle, *Sens. Actuators, B*, 2012, **168**, 442–445.
8 D. D. Carlo, K.-H Jeong and L. P. Lee, *Lab Chip*, 2003, **3**, 287–291.
9 S. Bhattacharya, S. Salamat, D. Morisette, P. Banada, D. Akin, Y.-S. Liu, A. K. Bhunia, M. Ladisch and R. Bashir, *Lab Chip*, 2008, **8**, 1130–1136.
10 N. Privorotskaya, Y. S. Liu, J. Lee, H. Zeng, J. A. Carlisle, A. Radadia, L. Millet, R. Bashir and W. P. King, *Lab Chip*, 2010, **10**, 1135–1141.
11 S. S. Rubakhin, E. V. Romanova, P. Nemes and J. V. Sweedler, *Nat. Methods*, 2011, **8**, S20–S29.
12 H. Lu, M. A. Schmidt and K. F. Jensen, *Lab Chip*, 2005, **5**, 23–29.
13 J. C. Weaver, *J. Cell. Biochem.*, 1993, **51**, 426–435.
14 B. Rubinsky, *Irreversible Electroporation*, Springer, Heidelberg, 2009.
15 J. A. Lundqvist, F. Sahlin, M. A. I. Åberg, A. Strömberg, P. S. Eriksson and O. Orwar, *Proc. Natl. Acad. Sci. U. S. A.*, 1998, **95**, 10356–10360.
16 M. Fox, D. Esveld, A. Valero, R. Luttge, H. Mastwijk, P. Bartels, A. van den Berg and R. Boom, *Anal. Bioanal. Chem.*, 2006, **385**, 474–485.
17 M. Khine, A. Lau, C. Ionescu-Zanetti, J. Seo and L. P. Lee, *Lab Chip*, 2005, **5**, 38–43.
18 M. Khine, C. Ionescu-Zanetti, A. Blatz, L.-P. Wang and L. P. Lee, *Lab Chip*, 2007, **7**, 457–462.
19 C. Xie, Z. Lin, L. Hanson, Y. Cui and B. Cui, *Nat. Nanotechnol.*, 2012, **7**, 185–190.
20 O. H. Elibol, B. Reddy Jr and R. Bashir, *Appl. Phys. Lett.*, 2008, **93**, 131908.
21 O. H. Elibol, B. Reddy Jr, P. R. Nair, B. Dorvel, F. Butler, Z. S. Ahsan, D. E. Bergstrom, M. A. Alam and R. Bashir, *Lab Chip*, 2009, **9**, 2789–2795.
22 B. Reddy Jr, O. H. Elibol, P. R. Nair, B. R. Dorvel, F. Butler, Z. Ahsan, D. E. Bergstrom, M. A. Alam and R. Bashir, *Anal. Chem.*, 2011, **83**, 888–895.
23 P. Bajaj, B. Reddy, L. Millet, C. Wei, P. Zorlutuna, G. Bao and R. Bashir, *Integr. Biol.*, 2011, **3**, 897–909.
24 S. Lindström, K. Mori, T. Ohashi and H. Andersson-Svahn, *Electrophoresis*, 2009, **30**, 4166–4171.
25 K. Ramser and D. Hanstorp, *J. Biophotonics*, 2010, **3**, 187–206.
26 S. Lindström and H. Andersson-Svahn, *Lab Chip*, 2010, **10**, 3363–3372.
27 T. Henighan, A. Chen, G. Vieira, A. J. Hauser, F. Y. Yang, J. J. Chalmers and R. Sooryakumar, *Biophys. J.*, 2010, **98**, 412–417.
28 G. Vieira, T. Henighan, A. Chen, A. J. Hauser, F. Y. Yang, J. J. Chalmers and R. Sooryakumar, *Phys. Rev. Lett.*, 2009, **103**, 128101.
29 G. Vieira, A. Chen, T. Henighan, J. Lucy, F. Y. Yang and R. Sooryakumar, *Phys. Rev. B: Condens. Matter Mater. Phys.*, 2012, **85**, 174440.
30 H. A. Svahn and A. Van Den Berg, *Lab Chip*, 2007, **7**, 544–546.
31 B. R. Dorvel, B. Reddy, J. Go, C. Duarte Guevara, E. Salm, M. A. Alam and R. Bashir, *ACS Nano*, 2012, **6**, 6150–6164.
32 C. Grosse and H. P. Schwan, *Biophys. J.*, 1992, **63**, 1632–1642.
33 B. Alberts, A. Johnson, J. Lewis, M. Raff, K. Roberts and P. Walter, *Molecular Biology of the Cell*, Garland Science, New York, NY, 2002.
34 M. M. Browne, G. V. Lubarsky, M. R. Davidson and R. H. Bradley, *Surf. Sci.*, 2004, **553**, 155–167.

